Supplementary materials

Contents:

- Materials and methods – additional detailed material and methods
- Tables (S1-S3 and S6) – Tables S4 and S5 are included as separate xlsx files
- Figures (S1-S7)
- References

Materials and methods

Study population

During 2014-2016, the Minnesota Veterinary Diagnostic Laboratory (MVDL) cultured and tested for antimicrobial susceptibility 1,597 isolates belonging to 75 nontyphoidal *Salmonella* (NTS) serotypes collected from swine clinical samples of multiple sources originating mainly from the U.S. Midwest (Illinois, Indiana, Iowa, Kansas, Michigan, Minnesota, Missouri, Nebraska, North Dakota, Ohio, South Dakota and Wisconsin). Isolates were routinely tested for antimicrobial susceptibility using a panel of 17 antimicrobials, including enrofloxacin and ceftiofur. Among them, 513 isolates (32.12%) belonging to 42 serotypes were resistant to either enrofloxacin (n=169), ceftiofur (n=191) or both (n=153). For the purpose of this study, a subset of 183 isolates of 17 NTS serotypes were conveniently selected based on their resistance profile (**Table S4**). These isolates were: i) resistant to either enrofloxacin (n=49), ceftiofur (n=30) or both (n=29); or (ii) susceptible to both (n=27). In addition, previously obtained WGS information for 48 *S.* 4,[5],12:i:- isolates: i) resistant to either enrofloxacin (n=7), ceftiofur (n=5) or both (n=4); or (ii) susceptible to both (n=32), cultured from swine samples from the Midwest during 2014-2015 (described in Elnekave et al. (1)), was included in this study. Overall, the selected isolates represented similar percentage of isolates from the Midwest (approximately 80%; **Table S6**) and of isolates collected during 2015 (approximately 80%) as was found among all 513 resistant isolates collected in the MVDL during that period (data not shown). In addition, the selected isolates represent different swine systems, farms, and locations within the systems (data not shown).

The initial number of isolates used for this study was 185. However, two isolates with low quality assemblies (see below; **Figure S1**) were removed and not included in the final analysis.

The sample processing of all study isolates (apart from the 48 *S.* 4,[5],12:i:- isolates from the previous study) was as follows: During 2014-2016, samples were recovered at the MVDL and antimicrobial susceptibility tests were conducted at the time of administration. Samples were then stored at minus 80°C until September 2017. Thawed isolates were streaked on MacConkey agar and a single colony was selected and grown in Luria-Bertani (LB) broth. DNA extraction was conducted using the DNEasy Blood & Tissue kit (Qiagen). Extracted DNA was then transferred to either the Minnesota Health Department (MDH; n=83) or the University of Minnesota Genomics Center (UMGC; n=54) for whole genome sequencing (WGS). Illumina MiSeq (2x250bp, paired-end reads) and Illumina HiSeq 2500 High-Output (2x125bp, paired-end reads) platforms were used for WGS at the MDH and UMGC, respectively.

Following assembly (below), in-silico serotyping was applied to all strains, using *Salmonella* In Silico Typing Resource (SISTR) platform (v1.0.2; (2)). The in-silico serotype in agreement between the three identification systems within SISTR was compared with the isolate serotype. In case of disagreement, the in-silico serotype was used (except for *S.* Typhimurium var 5-, which SISTR was not able to differentiate from *S.* Typhimurium). This approach was in agreement with the phylogeny (**Figure 1**).

Core genome alignment and phylogeny construction

For the purpose of phylogeny construction, the Single Nucleotide Polymorphism (SNP) detection was as described in detail by Elnekave et al. (1). The following thresholds were used for variant calling: coverage threshold of eight, a minimum average base quality (Pherd score) of 30, and a 90% agreement threshold.

Identification of resistance mechanisms

Paired-end Illumina reads were initially filtered, based on their quality, using FASTQC (v0.11.5; (3)) and *de-novo* genome assemblies were conducted using 'SPAdes' (v3.12.0; (4)) with the default setting. For estimating the contig quality we used QUAST (v4.6.3; (5)) and selected for further analysis only isolates with raw reads that resulted in assembled contigs with N50 of at least 30,000 nucleotides. In addition, we used Bowtie2 (v2.3.4.1; (6)) to align the raw reads to the contigs and BBmap (v38.06; (7)) to calculate the average coverage of the contigs. Only isolates with average coverage higher than 20 were further analyzed.

Multi Locus Sequence Types (MLST), plasmid replicon types and the presence of acquired antimicrobial resistance genes (AARGs) were determined using the webserver workflow of the 'bacterial analysis pipeline' at the Center of Genomic Epidemiology (https://cge.cbs.dtu.dk/services/cge/). For this purpose, the assembled contigs of each isolate were concatenated and then uploaded to the webserver, where the pipeline executes a workflow of the following services: Contig Analizer (v1.0), KmerFinder (v2.1; (8, 9)), ResFinder (v2.1; (10)), MLST (v1.6; (11)), PlasmidFinder (v1.2; (12)) and pMLST (v1.4; (12)). As the concatenated contigs of each isolate were used as an input, the CGE output was provided per isolate and not by the specific contigs of each isolate. We therefore had to use BLAST in order to localize the AARGs on specific contigs (see below).

In addition, mutations in quinolone target enzymes (*gyrA*, *gyrB*, *parC* and *parE*) and efflux pump regulation genes (*acrR*, *ramR*, *marR* and *soxR*) were identified using a local BLAST (v2.4.0+; (13)) as described in detail previously (1). Gene alignments were visualized using AliView software (v1.18; (14)).

For the purpose of this analysis, all chromosomal mutations were considered to be potentially contributing for resistance. However, for chromosomal mutations that were found in at least 15

isolates, we evaluated the associations between the detection of mutation and the phenotypic resistance to enrofloxacin using Fisher exact tests (statistically significant when $P < 0.05 / 7 = 0.007$ (Bonferroni's correction to account for multiple testing); **Table S3**). Non-significant associations between phenotypic resistance to enrofloxacin and the chromosomal mutations T717N in *gyrB* and T57S, S255T, S395N, A469S and T620A in *parC* were found and these mutations were excluded from the analyses.

Identification of the plasmids harboring AARGs

A local BLAST (v2.4.0+; (13)) was used to identify the contigs containing the AARG genes in each isolate (for this purpose, nucleotide fasta files were downloaded for the query genes from ResFinder (v2.1; (10)). These contigs were then BLASTed (online) against the NCBI repository (NCBI nt) and the first ten matches were recorded. Then, for each AARG, a matrix containing a list of contigs (each represent a single isolate, as none of the isolates harbored more than a single copy of an AARG) and their BLAST matches was created. We counted the total number of isolates in which a specific match was identified. Then, the accessions of all matches found to be present in at least 10% of the isolates for each AARG, were screened (using free-text search) on the NCBI 'GenBank' to identify matches from plasmids which also contain the AARG name or resistance to the AARG antimicrobial family. For this purpose the following search words were used: "plasmid"; "*qnr*"; "aac(6"; "*bla*" (including only bla_{CMY}, bla_{CTX} or bla_{SHV} genes); "resistance"; "cephalosporin" (with specific indication of extended spectrum resistance); and "quinolone". The plasmid sequences of the filtered BLAST matches were downloaded from NCBI (as FASTA files) and for each AARG, the raw short-reads of the isolates were aligned (using Bowtie2 v2.3.4.1; (6)) to these plasmid sequences. In these alignments, we took a

conservative approach and base locations with less than eight bases aligned (BEDTools v2.27.1 (15) was used to retrieve the coverage per location) were regarded as locations with coverage depth of zero. We then calculated the alignment's coverage breadth percentile using the following formula (1):

(1) coverage breadth (%) = 100 × (reference genome length - # of positions with zero coverage) / reference genome length

Therefore, the absolute coverage breadth formula was (2):

(2) absolute coverage breadth = (breadth coverage (%) × reference genome length)/100

Finally, for each AARG, the following information from each isolate mapped to a reference plasmid was summarized and compared: 1. coverage breadth (%), 2. absolute coverage breadth, 3. number of SNPs.

For each AARG gene, reference plasmids whose alignment had the highest coverage breadth percentage (top two) or highest absolute coverage breadth (top two) were selected out of the reference plasmid alignments in which at least 60% coverage breadth and less than 200 SNPs were found (SNPs were identified using SAMtools v1.9 (16) and VarScan v2.4.3 (17)). The selected reference plasmids were then considered as possible plasmid sequence containing the AARG. If similar alignment scores were obtained for multiple plasmids in the same isolate, all plasmids were grouped together (**Table S5**). In addition, in some cases, short plasmid references had high coverage depth percentage and a low number of SNPs. Yet when these short plasmid references were blasted against plasmid references with the high absolute coverage breadth that were identified in the same isolate, we found that certain regions in the small plasmid reference sequence were present in multiple locations along the longer reference plasmid sequence.

Therefore, these short reference plasmids were not regarded as possible plasmids and were excluded from the analysis.

In all analyses, the default settings were used for BLAST against the NCBI repository. Yet, for the local BLAST a threshold for positive detection was set to at least 90% identity and more than 60% coverage of the query sequence following the cutoffs used by ResFinder (v2.1; (10)).

In addition, we have screened (using free-text search) the U.S. Food and Drug Administration (FDA), NARMS Now (FDA. NARMS Now. Rockville, MD: U.S. Department of Health and Human Services; https://www.fda.gov/animalveterinary/safetyhealth/antimicrobialresistance/nationalantimicrobialresistancemonitoringsystem/ucm570685.htm. Accesed: 06/18/2018) surveillance program in slaugtherhouse findings to identify of 19 *Salmonella* isolates recovered from swine cecal samples between 2013 and 2015 that harbored *qnr*B19. Their raw-reads were downloaded and the plasmids were characterized based on the short-read assemblies (see manuscript for results). Three and ten of these isolates were previously described by Tyson et al. (18) as harboring plasmids in the sizes of 2,699bp and 3,071bp, respectively. Using our multi-step approach described above we identified plasmids from group I (including plasmids of 2,617 - 2,826bp) and group II (including plasmids of 3,071 - 3,082bp) for these three and ten isolates, respectively. The consistency between our findings and those reported by Tyson el al. (18) in independent analyses strengthens the validity of the approach taken here.

Pacific Biosciences (Pac-Bio) sequencing

Ten isolates were selected for Pacific Biosciences (Pac-Bio) sequencing based on their serotype and the plasmids that were identified in those using the short-read (illumina) assembly. Pac-Bio

sequencing provides long sequences, yet with high error rate (19). Therefore, LoRDEC v0.9 ((20); with k-mer size=19 and abundance threshold=2) was used for long-read error correction by mapping the Illumina short-reads to them and using the short-reads to correct unmapped regions along the path of the de Bruijn graph. Then a *de-novo* hybrid assembly was performed using Unicycler (v0.4.4; (21)) (with the default settings and depth filter=0.1%), using both Illumina short-reads and corrected Pac-Bio long-reads. Bandage (v0.8.1; (22)) was used for assembly visualization and a built-in BLAST (in Bandage) was used for detection of the AARGs and the plasmids harboring them. Short repetitive sequences (approximately 25bp long) were removed. For long-read plasmids smaller than 10,000bp, nodes with average coverage lower than 14 were removed. The final FASTA files containing the long-read plasmid sequences were then saved and used for further analyses. The plasmids identified via long-read assembly were then compared with the plasmids identified from short-read assemblies, using NCBI nucleotide megablast; and Blast Ring Image Generator (BRIG v0.95; (23)) was used for alignment visualization.

Data summarizing and statistical analysis

Data was summarized using Microsoft Excel and packages 'stringr' (v1.2.0; (24)), 'dplyr' (v0.7.4; (25)) and 'xlsx' (v0.5.7; (26)) in R (v3.4.3; (27)). Hmisc package (v4.1.1; (28)) was used for capitalizing the first letters in the serotype names. In addition, 'VennDiagram' package (v1.6.18; (29)) was used to create Venn diagrams and 'gridExtra' package (v2.3; (30)) for fitting multiple figures on one page.

In addition, collinearity between AARG pairs was assessed following Dohoo et al. (31) by creating 2X2 tables for each AARG pair and calculating the odd ratios. Odds ratio of 8-10 or

higher was considered as suggestive of collinearity (i.e. high correlation) between the AARG pairs.

Data Deposition

The raw-reads from the Illumina sequencing conducted at the MDH were deposited in the NCBI sequence read archive (SRA) under BioProject PRJNA215333. The raw-reads from the Illumina and Pac-Bio sequencing conducted at the UMGC were deposited in the NCBI sequence read archive (SRA) under BioProject PRJNA505665. The long-read assemblies of plasmids harboring AARGs were uploaded to GenBank (accessions MK191835 to MK191846). The isolate details are presented in **Table S4**.

Table S1 – Chromosomal genes in which mutations may lead to resistance to quinolones

Mechanism	Gene	Gene description	Gene coding sequences (CDS)*
Quinolone target enzymes	*gyrA*	DNA gyrase subunit A	NP_461214.1
	gyrB	DNA gyrase subunit B	NP_462735.1
	parC	DNA topoisomerase IV subunit A	NP_462089.1
	parE	DNA topoisomerase IV subunit B	NP_462096.1
Efflux pump regulation genes	*ramR*	Local repressor for *ramA* expression in *S*. Typhimurium	NP_459572.1†
	soxR	redox-sensitive transcriptional activator SoxR	NP_463131.1†
	marR	Transcriptional regulator	NP_460480.1†
	acrR	DNA-binding transcriptional repressor AcrR	NP_459472.1‡

*_Salmonella_ Typhimurium LT2 (NCBI accession number: NC_003197) served as the reference genome.

†Abouzeed et al. (32).

‡Olliver et al. (33).

Table S2 – Genetic resistance mechanisms (i.e. presence of acquired antimicrobial resistance genes (AARGs) and mutations in target enzymes and the efflux pump regulation genes) which may result in resistance to enrofloxacin, summarized by nontyphoidal *Salmonella* (NTS) serotypes and phenotypic resistance to enrofloxacin.

NTS serotype	Resistance to enrofloxacin (MIC≥1mg/L)	n	Presence of AARGs (no.)	Mutations* which may result in resistance to enrofloxacin† (no.)				
				Target enzymes‡			Efflux pumps regulation	
				gyrA	*gyrB*	*parC*	*ramR*	others
Agona	No	8			T717N (8)	T57S (8), S395N (8), T620A (8)	(2)§	
	Yes	14	*qnrB19* (1), *qnrB2* (1)	S83Y (11)	T717N (14)	T57S (14), S80R (1), S395N (14), T620A (14)	A37T (1), Q19L (1), (11)§, (1)¶	
Alachua	Yes	7	qnrB15-like (1), *qnrB19* (6)	D87G (1), S83F (1)		T57S (7), S255T (7), S395N (7), A469S (7), T620A (7)	(7)#	V213F (7)††, S216P (7)††
Bovismorbific-ans	No	1				T57S (1), S395N (1), A469S (1), T620A (1)		N214T (1)††, P217R (1)††
Braenderup	No	1	*qnrB2* (1), (1)**	R413L (1)		T57S (1)		
Brandenburg	No	4				T57S (4), S395N (4), T620A (4)	Y92H (1), (1)#	N214T (4)††
	Yes	2	*qnrB2* (1), (1)**	S83L (1)		E51D (1), T57S (2), S395N (2), T620A (2)	(2)#	N214T (2)††
Derby	No	4				T57S (4), A469S (4), T620A (4)		S216A (4)††
Heidelberg	No	2				T57S (2), S395N (2), A469S (2), T620A (2)		
	Yes	12	*qnrB19* (8), *qnrB19*-like (1), *qnrD* (1)	D87N (2), S83Y (1)		T57S (12), S395N (12), A469S (12), T620A (12)	H99P (1), I55T (1), (3)#	
Infantis	No	3			Q624K (3)	T57S (3), S395N (3), A469S (3), T620A (3)		
	Yes	1	*qnrB2* (1)		Q624K (1)	T57S (1), S395N (1), A469S (1), T620A (1)		
London	No	1				T57S (1), S255T (1), S395N (1), A469S (1), T620A (1)	M83T (1)	
	Yes	3	*qnrB19* (3)			T57S (3), S255T (3), S395N (3), A469S (3), T620A (3)	M83T (3)	
4,[5],12:i:-	No	41	*qnrB19*-like (1), *qnrB2* (1), (1)**		T616I (1)		W89L (1), (2)#	V110L (1)‡‡
	Yes	17	*qnrB19* (11), *qnrB2* (6), *qnrS1* (1) ,(2)**	S83F (1)			G180E (1), W89R (1), (1)#	
Muenchen	No	2		A873V (1)		T57S (2), S255T (1), R365L (1), S395N (2), A469S (2), T620A (2)		
	Yes	1	*qnrB19* (1)	A873V (1)		T57S (1), S255T (1), R365L (1), S395N (1), A469S (1), T620A (1)	(1)#	
Ohio	No	1				T57S (1), S395N (1)	A15T (1)	G15D (1)§§
Rissen	No	1				T57S (1), S255T (1), S395N (1), A469S (1), T620A (1)		
	Yes	2	*qnrB19* (1) , (1)**	D87N (1)		T57S (2), S255T (2), S395N (2), A469S (2), T620A (2)	L115F (1)	C148F (1)††

Senftenberg	No	1		D87N (1)		T57S (1), A469S (1), T620A (1)		
	Yes	2	*qnrB19* (1), *qnrB2* (1) ,(1)**			T57S (2), A469S (2), T620A (2)	(1)#	
Typhimurium var 5-	No	7					A149T (1)	
	Yes	18	qnrB15-like (1), *qnrB19* (11), *qnrB2* (2), *qnrS2* (1)	D87N (4), S83F (1)		S80I (3)	A40T (3), R102L (1), G96D (1), H99Q (1), T18P (2), P100T (1), (1)#	
Typhimurium	No	15	*qnrB19* (1), *qnrB19*-like (3)	D830N (1)			H99Q (1), P100T (1)	
	Yes	4	*qnrB19* (3), *qnrB2* (1) ,(1)**				(1)#	
Worthington	No	2				T57S (2), S395N (2), A469S (2), T620A (2)		
	Yes	6	qnrB15-like (2),*qnrB2*-like (1), *qnrB19* (2), *qnrB19*-like (2)			T57S (6), S395N (6), A469S (6), T620A (6)	(2)#	

215

216 *Non-synonymous mutations. Those potentially associated with resistance to enrofloxacin are

217 underscored (see manuscript, supplementary materials text and **Table S3** for clarification).

218 †Mutation locations indicated according to the amino acid (AA) location following the scheme:

219 ['original AA'][location]['new AA']. Amino acids are presented using single letter abbreviation.

220 ‡No mutations were found in *parE*.

221 §*ramR* was not detected.

222 ¶insertion of one nucleic acid resulting in multiple stop codons in *ramR*.

223 #deletion of up to 45 amino acids in *ramR*.

224 **presence of *aac(6')Ib-cr*-like.

225 ††mutation in *acrR*.

226 ‡‡mutation in *soxR*.

227 §§mutation in *marR*.

228

229

Table S3 – list of the chromosomal mutations in the target enzymes and efflux pump regulating genes that were found in this study.

Gene		Mutations	QRDR*	All isolates		Only serotypes in which the mutation was found†		
				Resistant (no./Total (%))	Susceptible (no./Total (%))	Resistant (no./Total (%))	Susceptible (no./Total (%))	Reference
Target enzymes	*gyrA*	S83F	Yes	3/89 (3.4)	0/94 (0)			(34-36)
		S83L	Yes	1/89 (1.1)	0/94 (0)			(37)
		S83Y	Yes	12/89 (13.5)	0/94 (0)			(34, 36)
		D87G	Yes	1/89 (1.1)	0/94 (0)			(34, 36, 37)
		D87N	Yes	7/89 (7.9)	1/94 (1.1)			(34-37)
		R413L	No	0/89 (0)	1/94 (1.1)			NA
		D830N	No	0/89 (0)	1/94 (1.1)			NA
		A873V	No	1/89 (1.1)	1/94 (1.1)			NA
	gyrB	T616I	No	0/89 (0)	1/94 (1.1)			NA
		Q624K	No	1/89 (1.1)	3/94 (3.2)			NA
		T717N‡	No	14/89 (15.7)	8/94 (8.5)	14/14 (100)	8/8 (100)	NA
	parC	E51D	No	1/89 (1.1)	0/94 (0)			NA
		T57S‡	Yes	50/89 (56.2)	31/94 (33)	50/50 (100)	31/31 (100)	(34, 37)
		S80I	Yes	3/89 (3.4)	0/94 (0)			(34)
		S80R	Yes	1/89 (1.1)	0/94 (0)			(34)
		S255T‡	No	13/89 (14.6)	3/94 (3.2)	13/13 (100)	3/4 (75)	NA
		R365L	No	1/89 (1.1)	1/94 (1.1)			NA
		S395N‡	No	48/89 (53.9)	25/94 (26.6)	48/48 (100)	25/25 (100)	NA
		A469S‡	No	34/89 (38.2)	17/94 (18.1)	34/34 (100)	17/17 (100)	NA
		T620A‡	No	50/89 (56.2)	29/94 (30.9)	50/50 (100)	29/29 (100)	NA
	parE	-	-	-	-			-
Efflux pump regulating genes	*acrR*	C148F	NA	1/89 (1.1)	0/94 (0)			NA
		V213F	NA	7/89 (7.9)	0/94 (0)			NA
		N214T	NA	2/89 (2.2)	5/94 (5.3)			NA
		S216P	NA	7/89 (7.9)	0/94 (0)			NA
		S216A	NA	0/89 (0)	4/94 (4.3)			NA
		P217R	NA	0/89 (0)	1/94 (1.1)			NA
	ramR	A15T	NA	0/89 (0)	1/94 (1.1)			NA
		T18P	NA	2/89 (2.2)	0/94 (0)			NA
		Q19L	NA	1/89 (1.1)	0/94 (0)			NA
		A37T	NA	1/89 (1.1)	0/94 (0)			NA
		A40T	NA	3/89 (3.4)	0/94 (0)			NA
		I55T	NA	1/89 (1.1)	0/94 (0)			NA
		M83T	NA	3/89 (3.4)	1/94 (1.1)			NA
		W89L	NA	0/89 (0)	1/94 (1.1)			NA

		W89R	NA	1/89 (1.1)	0/94 (0)			NA
		Y92H	NA	0/89 (0)	1/94 (1.1)			NA
		G96D	NA	1/89 (1.1)	0/94 (0)			NA
		H99P	NA	1/89 (1.1)	0/94 (0)			NA
		H99Q	NA	1/89 (1.1)	1/94 (1.1)			NA
		P100T	NA	1/89 (1.1)	1/94 (1.1)			NA
		R102L	NA	1/89 (1.1)	0/94 (0)			NA
		L115F	NA	1/89 (1.1)	0/94 (0)			NA
		A149T	NA	0/89 (0)	1/94 (1.1)			NA
		G180E	NA	1/89 (1.1)	0/94 (0)			NA
		Deletion[§]	NA	19/89 (21.3)	3/94 (3.2)	19/68 (23.5)	3/74 (4.05)	(38)
		Gene not found	NA	11/89 (12.4)	2/94 (2.1)			In isolate 44 we found only 35% of the gene in hybrid assembly. Similarly Akiyama et al. (38) described 315bp deletion in this gene
		Insertion[¶]	NA	1/89 (1.1)	0/94 (0)			NA
	marR	G15D	NA	0/89 (0)	1/94 (1.1)			NA
	soxR	V110L	NA	0/89 (0)	1/94 (1.1)			NA

[*]the Quinolone Resistance Determining Regions (QRDRs) for *gyrA* (70-152), *gyrB* (415-470) and *parC* (47-133) were defined according to Eaves et al. (36).

[†]Including only mutations that were found in at least 15 isolates. The total number of resistance and susceptible isolates out of the number of the total isolates in the serotypes in which the mutation was found.

[‡]not regarded as contributing the resistance. P >0.007, when including only serotypes in which this mutation was found (Fisher exact test with Bonferroni's correction).

[§]amino acid deletions - different positions. Regarded as contributing to enrofloxacin-resistance. P<0.007, when including only serotypes in which deletions were found (Fisher exact test with Bonferroni's correction).

¶the nucleotide Adenine is inserted in location 25 ->result in 3 stop codons.

Table S6 – The distribution of the nontyphoidal *Salmonella* (NTS) isolates included in this study, summarized by state

State	n / total (%)
Alaska	1 / 183 (0.55)
Alabama	1 / 183 (0.55)
Arkansas	1 / 183 (0.55)
Colorado	2 / 183 (1.09)
Iowa	25 / 183 (13.66)
Illinois	16 / 183 (8.74)
Indiana	1 / 183 (0.55)
Kansas	18 / 183 (9.84)
Minnesota	61 / 183 (33.33)
Missouri	7 / 183 (3.83)
North Carolina	1 / 183 (0.55)
Nebraska	14 / 183 (7.65)
Ohio	3 / 183 (1.64)
Oklahoma	20 / 183 (10.93)
Pennsylvania	1 / 183 (0.55)
Texas	10 / 183 (5.46)
Wisconsin	1 / 183 (0.55)

Figure S1 –

A schematic diagram illustrating the approach applied in this study

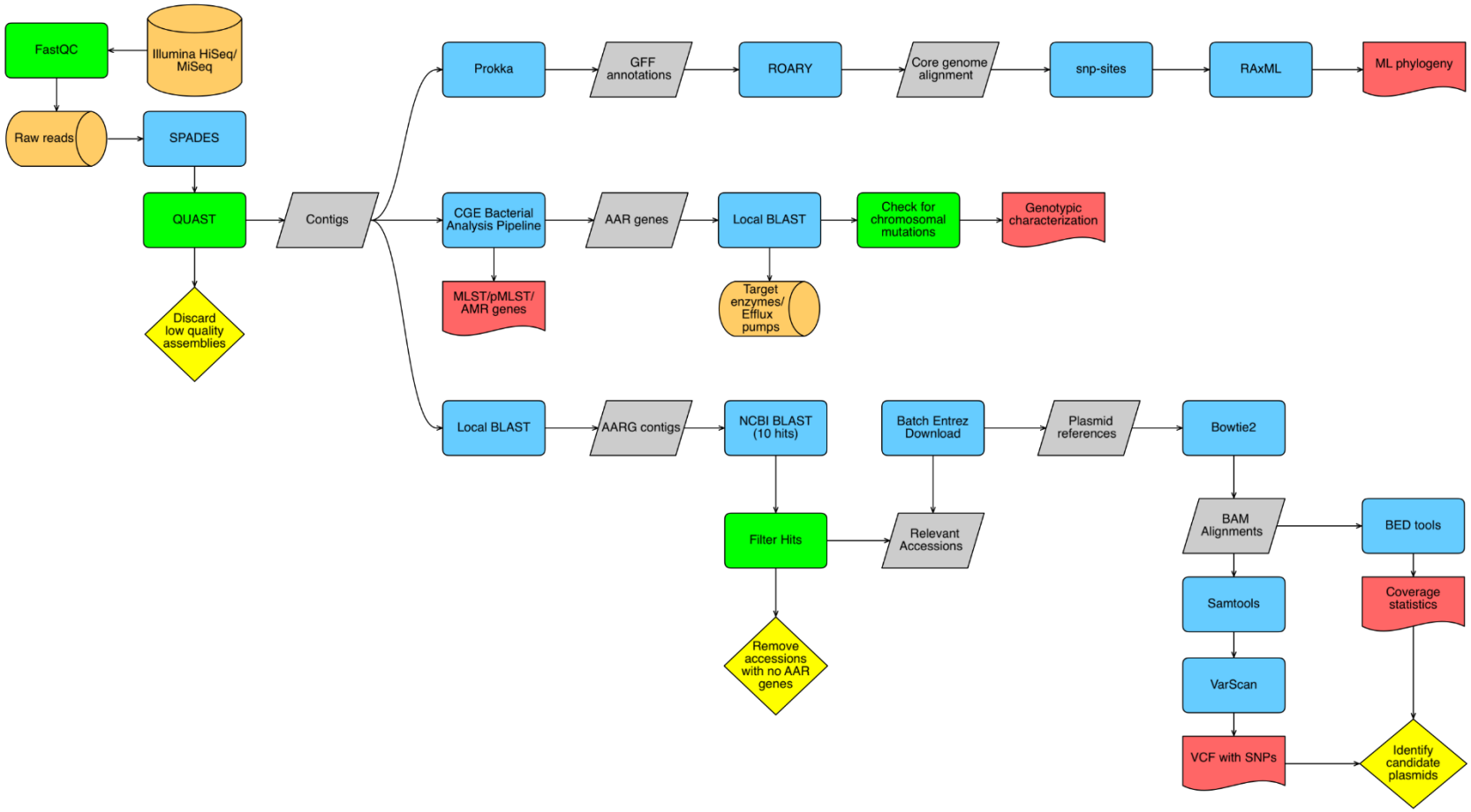

Figure S2 –

A BLAST ring alignment for short-read (Illumina) assembly plasmids and long-read (Pac-Bio) assembly plasmids harboring the *qnrD* (indicated in red). The percentage of identity for each aligned sequence with the reference plasmid (KF498970.1; inner black circle) is indicated on the legend.

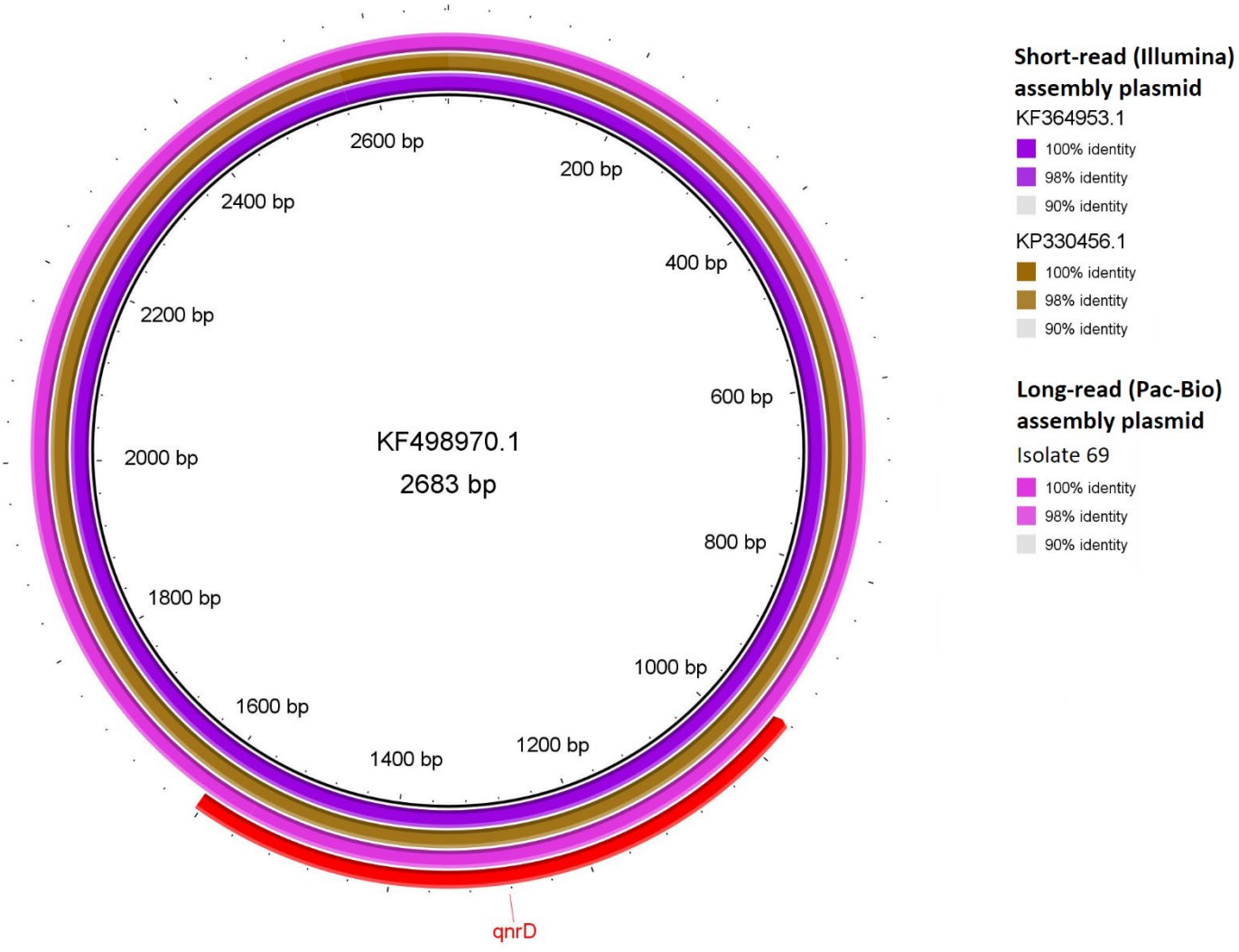

Figure S3 –

A BLAST ring alignment for short-read (Illumina) assembly plasmids with the long-read (Pac-Bio) assembly plasmid (Isolate_63) harboring the *qnrS2* (indicated in red). The percentage of identity for each aligned sequence with the reference plasmid (Isolate_65; inner black circle) is indicated on the legend.

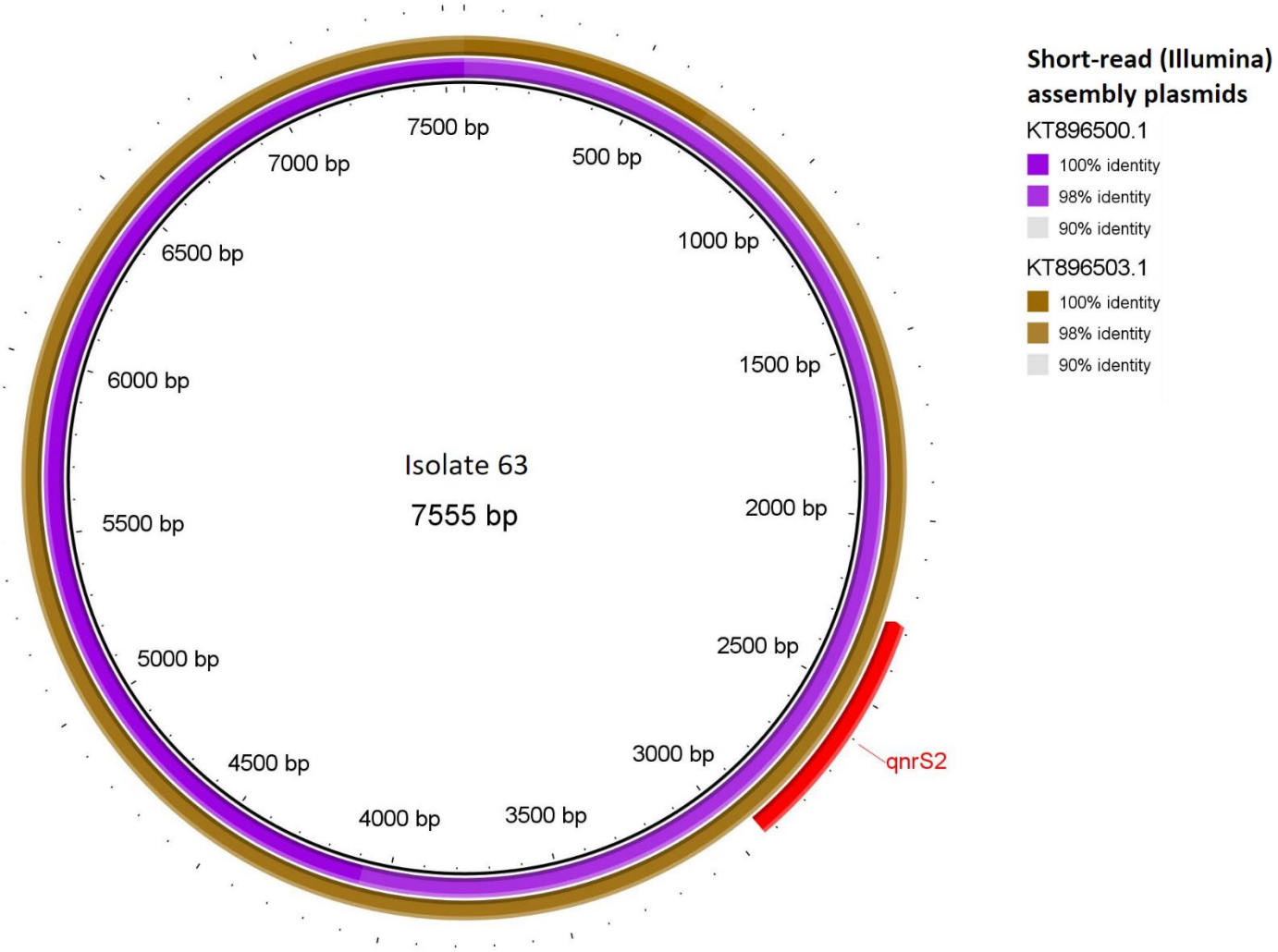

Figure S4 –

A BLAST ring alignment for short-read (Illumina) assembly plasmids and long-read (Pac-Bio) assembly plasmids harboring the *bla*$_{\text{CTX-M-27}}$ (indicated in yellow). The percentage of identity for each aligned sequence with the reference plasmid (EU855788.1; inner black circle) is indicated on the legend (*In the reference EU855788.1, *bla*$_{\text{CTX-M-14}}$ was detected in the same location and not *bla*$_{\text{CTX-M-27}}$).

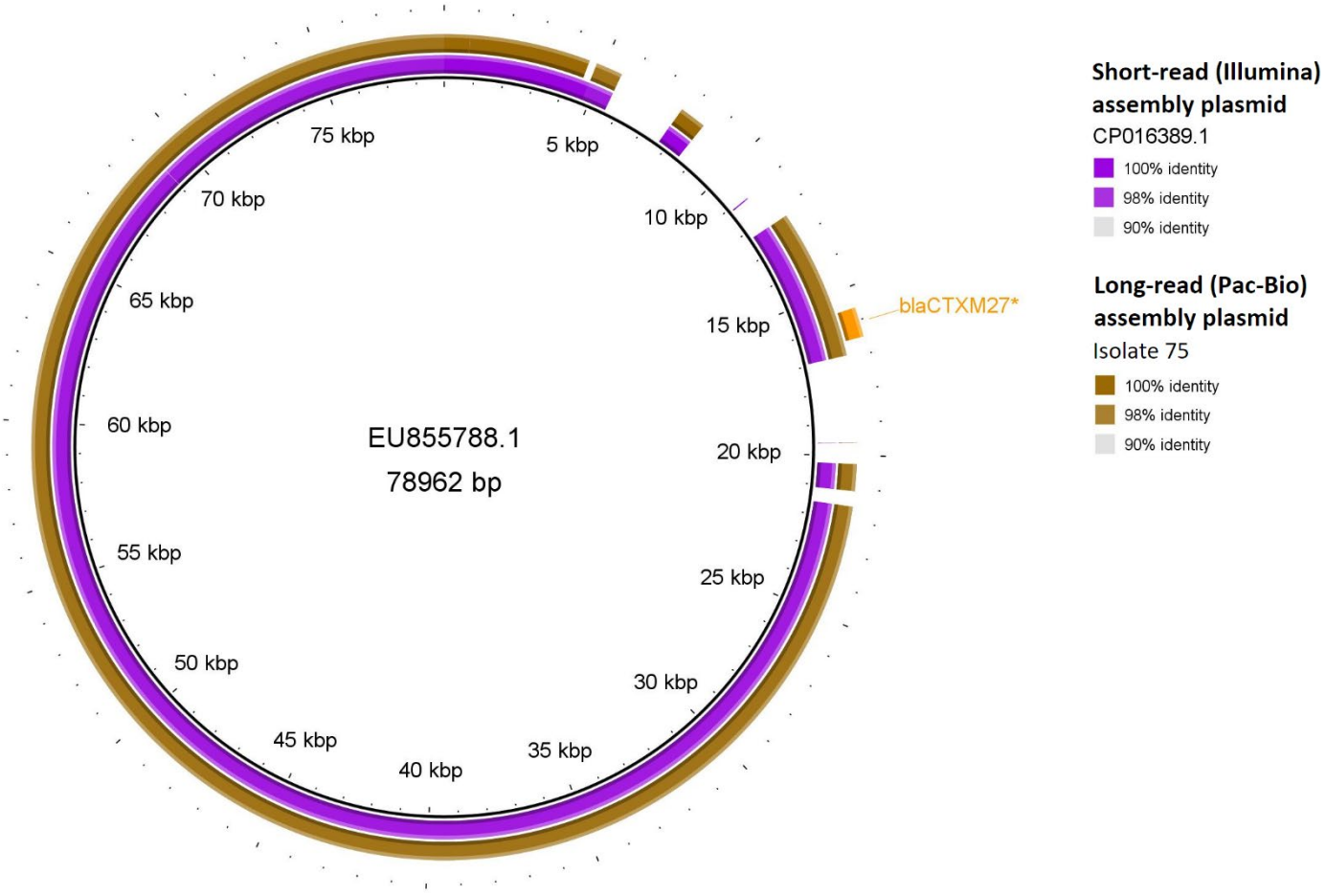

Figure S5 –

A BLAST ring alignment for short-read (Illumina) assembly plasmids and long-read (Pac-Bio) assembly plasmids harboring the *bla*$_{\text{CMY-2}}$ (indicated in yellow) in short-read assembly plasmids of group I. The percentage of identity for each aligned sequence with the reference plasmid (KP056256.1; inner black circle) is indicated on the legend.

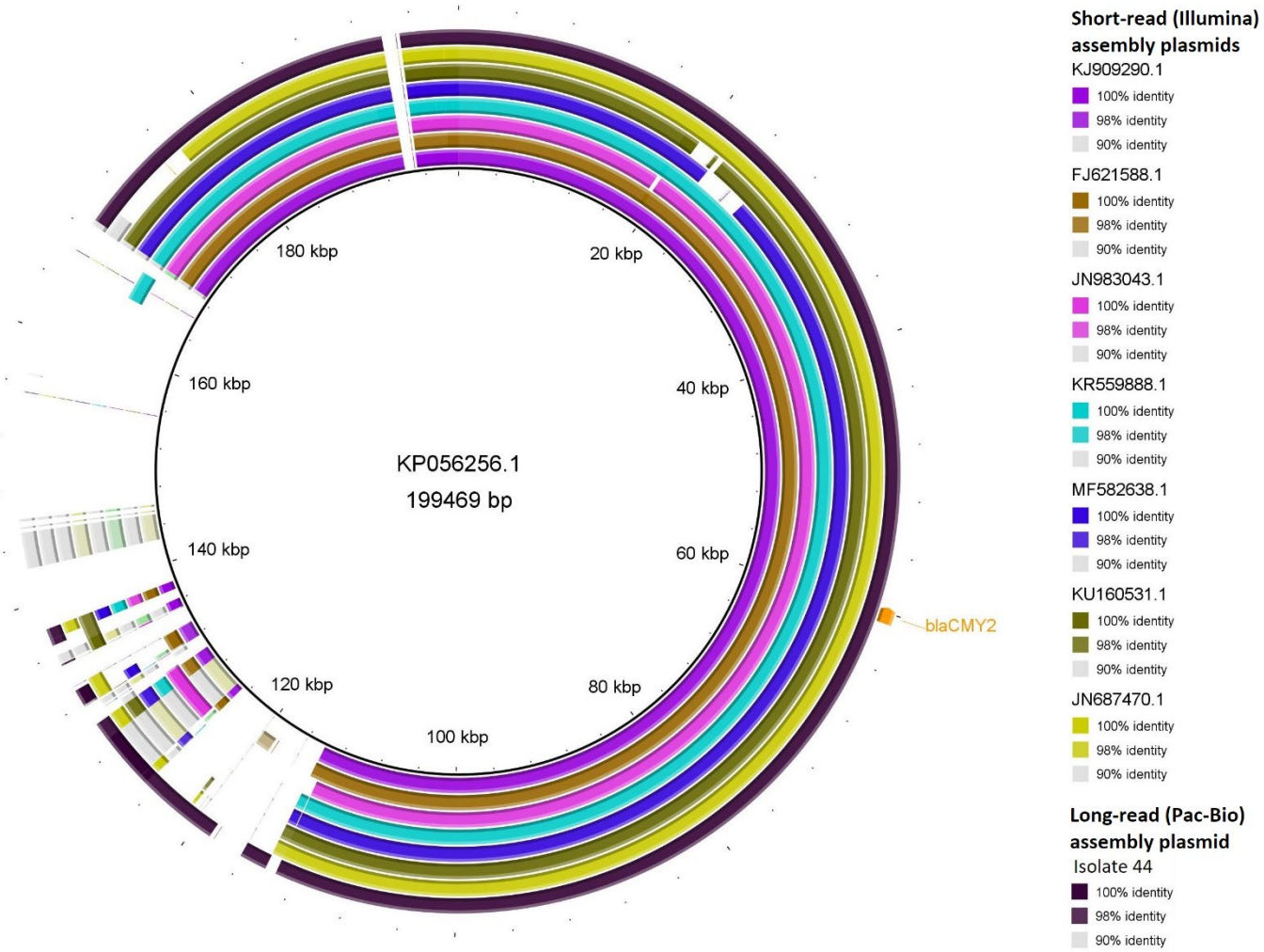

Figure S6 –

A BLAST ring alignment for short-read (Illumina) assembly plasmids and long-read (Pac-Bio) assembly plasmids harboring the *bla*$_{CMY-2}$ (indicated in yellow) in short-read assembly plasmids of group II. The percentage of identity for each aligned sequence with the reference plasmid (CP022064.1; inner black circle) is indicated on the legend.

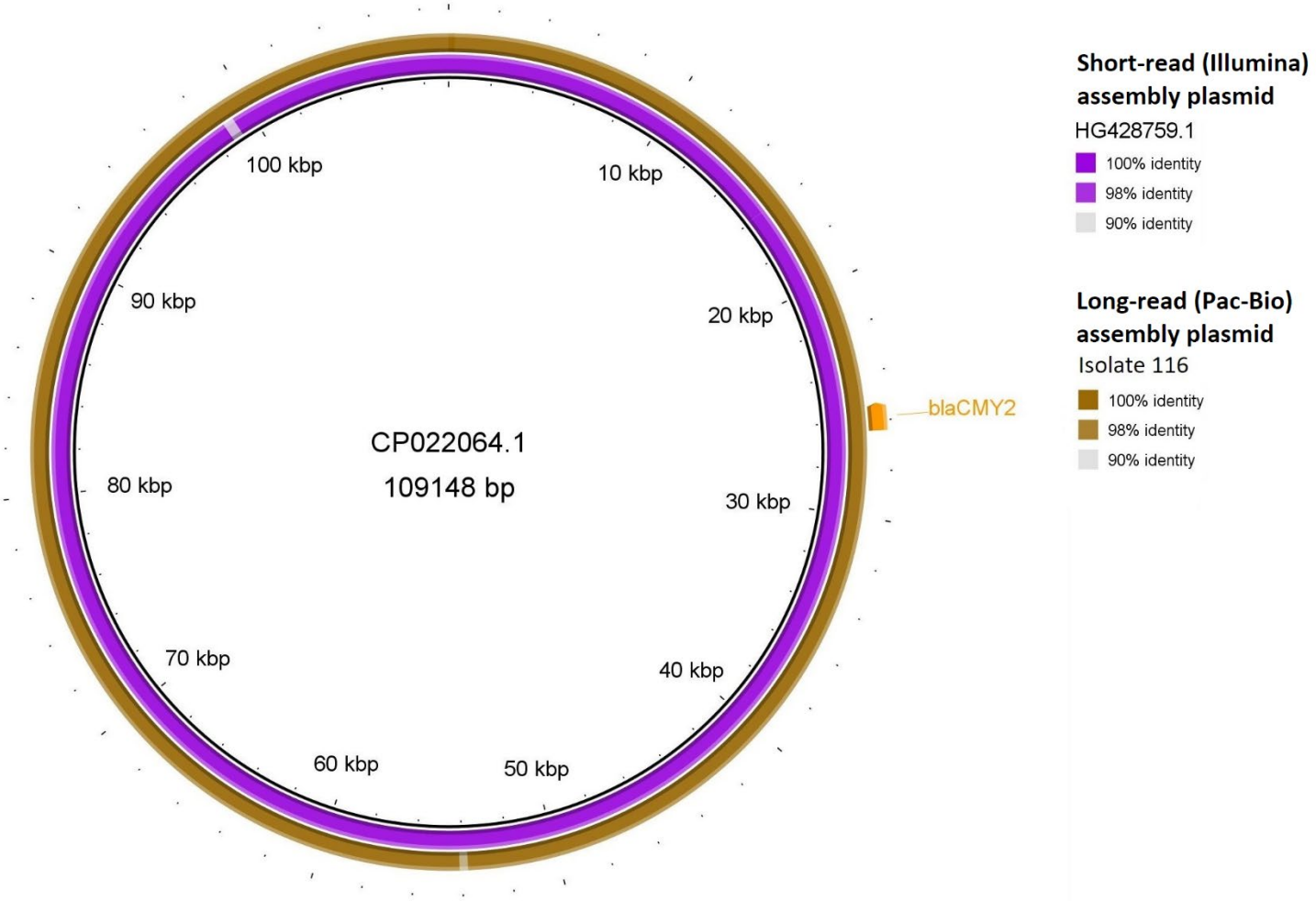

Figure S7 –

A BLAST ring alignment for short-read (Illumina) assembly plasmids and long-read (Pac-Bio) assembly plasmids harboring the *qnrB2*, *aac(6')Ib-cr* and *bla*$_{SHV-12}$ (indicated in the external circle in red, black and yellow, respectively). The percentage of identity for each aligned sequence with the reference plasmid (CP022064.1; inner black circle) is indicated on the legend.

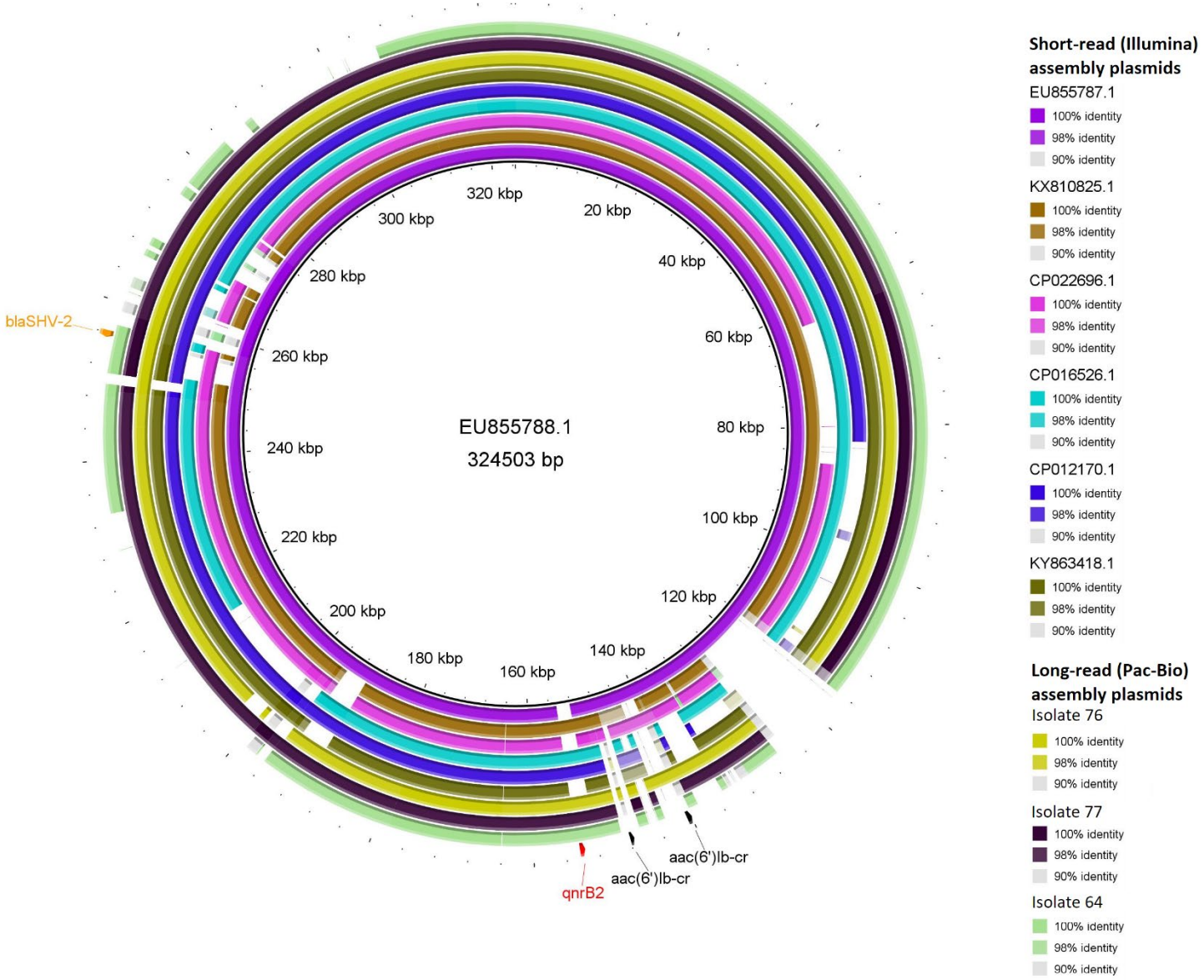

References

1. Elnekave E, Hong S, Mather AE, Boxrud D, Taylor AJ, Lappi V, Johnson TJ, Vannucci F, Davies P, Hedberg C, Perez A, Alvarez J. 2018. Salmonella enterica Serotype 4,[5],12:i:- in Swine in the United States Midwest: An Emerging Multidrug-Resistant Clade. Clin Infect Dis 66:877-885.
2. Yoshida CE, Kruczkiewicz P, Laing CR, Lingohr EJ, Gannon VP, Nash JH, Taboada EN. 2016. The Salmonella In Silico Typing Resource (SISTR): An Open Web-Accessible Tool for Rapidly Typing and Subtyping Draft Salmonella Genome Assemblies. PLoS One 11:e0147101.
3. Andrews S. 2010. FastQC: a quality control tool for high throughput sequence data. http://www.bioinformatics.babraham.ac.uk/projects/fastqc. Accessed
4. Bankevich A, Nurk S, Antipov D, Gurevich AA, Dvorkin M, Kulikov AS, Lesin VM, Nikolenko SI, Pham S, Prjibelski AD, Pyshkin AV, Sirotkin AV, Vyahhi N, Tesler G, Alekseyev MA, Pevzner PA. 2012. SPAdes: a new genome assembly algorithm and its applications to single-cell sequencing. J Comput Biol 19:455-77.
5. Gurevich A, Saveliev V, Vyahhi N, Tesler G. 2013. QUAST: quality assessment tool for genome assemblies. Bioinformatics 29:1072-5.
6. Langmead B, Trapnell C, Pop M, Salzberg SL. 2009. Ultrafast and memory-efficient alignment of short DNA sequences to the human genome. Genome Biol 10:R25.
7. Bushnell B. 2016. BBMap short-read aligner, and other bioinformatics tools, http://sourceforge.net/projects/bbmap/.

8. Hasman H, Saputra D, Sicheritz-Ponten T, Lund O, Svendsen CA, Frimodt-Moller N, Aarestrup FM. 2014. Rapid whole-genome sequencing for detection and characterization of microorganisms directly from clinical samples. J Clin Microbiol 52:139-46.
9. Larsen MV, Cosentino S, Lukjancenko O, Saputra D, Rasmussen S, Hasman H, Sicheritz-Ponten T, Aarestrup FM, Ussery DW, Lund O. 2014. Benchmarking of methods for genomic taxonomy. J Clin Microbiol 52:1529-39.
10. Zankari E, Hasman H, Cosentino S, Vestergaard M, Rasmussen S, Lund O, Aarestrup FM, Larsen MV. 2012. Identification of acquired antimicrobial resistance genes. J Antimicrob Chemother 67:2640-4.
11. Larsen MV, Cosentino S, Rasmussen S, Friis C, Hasman H, Marvig RL, Jelsbak L, Sicheritz-Ponten T, Ussery DW, Aarestrup FM, Lund O. 2012. Multilocus sequence typing of total-genome-sequenced bacteria. J Clin Microbiol 50:1355-61.
12. Carattoli A, Zankari E, Garcia-Fernandez A, Voldby Larsen M, Lund O, Villa L, Moller Aarestrup F, Hasman H. 2014. In silico detection and typing of plasmids using PlasmidFinder and plasmid multilocus sequence typing. Antimicrob Agents Chemother 58:3895-903.
13. Altschul SF, Gish W, Miller W, Myers EW, Lipman DJ. 1990. Basic local alignment search tool. J Mol Biol 215:403-10.
14. Larsson A. 2014. AliView: a fast and lightweight alignment viewer and editor for large datasets. Bioinformatics 30:3276-8.
15. Quinlan AR, Hall IM. 2010. BEDTools: a flexible suite of utilities for comparing genomic features. Bioinformatics 26:841-2.

16. Li H, Handsaker B, Wysoker A, Fennell T, Ruan J, Homer N, Marth G, Abecasis G, Durbin R, Genome Project Data Processing S. 2009. The Sequence Alignment/Map format and SAMtools. Bioinformatics 25:2078-9.
17. Koboldt DC, Zhang Q, Larson DE, Shen D, McLellan MD, Lin L, Miller CA, Mardis ER, Ding L, Wilson RK. 2012. VarScan 2: somatic mutation and copy number alteration discovery in cancer by exome sequencing. Genome Res 22:568-76.
18. Tyson GH, Tate HP, Zhao S, Li C, Dessai U, Simmons M, McDermott PF. 2017. Identification of Plasmid-Mediated Quinolone Resistance in Salmonella Isolated from Swine Ceca and Retail Pork Chops in the United States. Antimicrob Agents Chemother 61.
19. Ross MG, Russ C, Costello M, Hollinger A, Lennon NJ, Hegarty R, Nusbaum C, Jaffe DB. 2013. Characterizing and measuring bias in sequence data. Genome Biol 14:R51.
20. Salmela L, Rivals E. 2014. LoRDEC: accurate and efficient long read error correction. Bioinformatics 30:3506-14.
21. Wick RR, Judd LM, Gorrie CL, Holt KE. 2017. Unicycler: Resolving bacterial genome assemblies from short and long sequencing reads. PLoS Comput Biol 13:e1005595.
22. Wick RR, Schultz MB, Zobel J, Holt KE. 2015. Bandage: interactive visualization of de novo genome assemblies. Bioinformatics 31:3350-2.
23. Alikhan NF, Petty NK, Ben Zakour NL, Beatson SA. 2011. BLAST Ring Image Generator (BRIG): simple prokaryote genome comparisons. BMC Genomics 12:402.
24. Wickham H. 2015. stringr: Simple, Consistent Wrappers for Common String Operations. https://CRAN.R-project.org/package=stringr. Accessed
25. Wickham H, Francois, R., Henry, L., Müller, K. 2017. dplyr: A Grammar of Data Manipulation. R package version 0.7.4, https://CRAN.R-project.org/package=dplyr.

26. Dragulescu AA. 2014. xlsx: Read, write, format Excel 2007 and Excel 97/2000/XP/2003 files. R package version 0.5.7, https://CRAN.R-project.org/package=xlsx.
27. R Core Team. 2016. R: A language and environment for statistical computing, Vienna, Austria. https://www.R-project.org/.
28. Frank E. 2018. Hmisc: Harrell Miscellaneous. R package version 4.1-1, https://CRAN.R-project.org/package=Hmisc.
29. Chen H, Boutros PC. 2011. VennDiagram: a package for the generation of highly-customizable Venn and Euler diagrams in R. BMC Bioinformatics 12:35.
30. Auguie B. 2012. gridExtra: functions in Grid graphics. R package version 23 1.
31. Dohoo IR, Martin, S.W., Stryhn, H. 2012. Linear Regression, p 359-400, Methods in Epidemiologic Research. VER Inc., Charlottetown, Prince EdwardIsland, Canada.
32. Abouzeed YM, Baucheron S, Cloeckaert A. 2008. ramR mutations involved in efflux-mediated multidrug resistance in Salmonella enterica serovar Typhimurium. Antimicrob Agents Chemother 52:2428-34.
33. Olliver A, Valle M, Chaslus-Dancla E, Cloeckaert A. 2004. Role of an acrR mutation in multidrug resistance of in vitro-selected fluoroquinolone-resistant mutants of Salmonella enterica serovar Typhimurium. FEMS Microbiol Lett 238:267-72.
34. Hopkins KL, Davies RH, Threlfall EJ. 2005. Mechanisms of quinolone resistance in Escherichia coli and Salmonella: recent developments. Int J Antimicrob Agents 25:358-73.
35. Capoor MR, Nair D, Walia NS, Routela RS, Grover SS, Deb M, Aggarwal P, Pillai PK, Bifani PJ. 2009. Molecular analysis of high-level ciprofloxacin resistance in Salmonella enterica serovar Typhi and S. Paratyphi A: need to expand the QRDR region? Epidemiol Infect 137:871-8.

418 36. Eaves DJ, Randall L, Gray DT, Buckley A, Woodward MJ, White AP, Piddock LJ. 2004.
419 Prevalence of mutations within the quinolone resistance-determining region of gyrA, gyrB,
420 parC, and parE and association with antibiotic resistance in quinolone-resistant Salmonella
421 enterica. Antimicrob Agents Chemother 48:4012-5.
422 37. Wasyl D, Hoszowski A, Zajac M. 2014. Prevalence and characterisation of quinolone
423 resistance mechanisms in Salmonella spp. Vet Microbiol 171:307-14.
424 38. Akiyama T, Khan AA. 2012. Molecular characterization of strains of fluoroquinolone-
425 resistant Salmonella enterica serovar Schwarzengrund carrying multidrug resistance isolated
426 from imported foods. J Antimicrob Chemother 67:101-10.

427